

**ANALYSIS of GRANULAR FLOW USING MAGNETIC
RESONANCE IMAGING**

Lisa Bauer

2008 NSF/REU Program

Physics Department, University of Notre Dame

Advisor: Dr. Igor Veretennikov

ABSTRACT

In spite of their industrial and geological significance, the behavior of granular materials is not well understood, and an exact characterization as solids or liquids is inaccurate. This experiment was designed to study granular flow around a sphere, comparing observations to analytical solutions for viscous and inviscid fluid flow. A plunger was withdrawn through a cylinder of seeds in varying increments, acquiring images at each step using magnetic resonance imaging. Particle Image Velocimetry computed seed displacements, and averaging procedures showed the most common properties of motion. Although the observed granular flow did not closely resemble either viscous or inviscid fluid flow, it was evident that flow mechanisms were markedly different for plunging and withdrawal motions.

INTRODUCTION

Anyone who has ever built a sandcastle or played Hacky Sack is familiar with granular materials. These distinct, solid particles have an array of interesting characteristics, as they are unable to be classified as strict solids or liquids. Their behavior is not well understood, despite their importance in pharmaceuticals, construction and agriculture. Granular materials have several implications in geology, from sedimentation to landslides and avalanches.

It is difficult to understand the dynamics of a granular system. The mass of individual particles is so large that Classical Mechanics, and not Quantum Mechanics, would apply, and thermal energy, $k_B T$, is too small to overcome potential energy barriers. Fluid-like behavior is a dynamic phenomenon, and granular flow is non-Newtonian. As soon as the top layer in pile of granular materials exceeds the "angle of repose," an avalanche occurs within a finite-depth boundary layer at the pile's surface. The bulk of the material does not experience any motion [1].

However, granular materials can flow like liquids, and models developed to describe granular flow are referred to as granular hydrodynamics. Development of these models is often based on ideal dense, slow flows or rapid flows. Granular materials often show both of these flows at the same time, but in different spatial domains, and so a concern is how to model both flows, and the transition between them, accurately [2].

Another intriguing aspect of granular materials is the dilatancy phenomenon, or the need for granular material to expand before it can flow. Densely packed materials must make room for passing particles in order to flow [1]. Granular materials have a tendency to exhibit vaulting similar, as H.M. Jaeger and Sidney Nagel put it, to placing a keystone at the top of an arch. The natural occurrence of arches, as well as the inhomogeneity of granular material, leads to a nonuniform force network [1]. Since forces depend on compression at contact points, small displacements of even a single particle can produce large changes in the force network [3]. This is especially noticeable in collapses due to small displacements of the plunger in this experiment, and consequences will be discussed later in this paper.

METHOD

Experimental Apparatus

Magnetic resonance imaging (MRI) provided a non-invasive method of monitoring granular materials. Unlike using intrusive tracer particles, MRI allowed a thorough observation of motion in the desired area without disturbing granular flow. Rather than being reduced to studying surface effects, motion near the moving sphere was observed by carefully selecting image slices. Seeds were used as granular material, as their oil was able to produce a sufficient signal.

This experiment was aimed at studying the motion of granular materials in response to the withdrawal of sphere. The apparatus used for this experiment was placed inside the bore of a 7.0 T, 300 MHz, Bruker vertical-bore MRI system (see Figure 1). A cylinder 6.0 cm in diameter contained the seeds for each particular trial, and was placed inside the RF coil. A 0.38" acrylic sphere connected to a thin acrylic shaft formed the plunger. This plunger was attached to a long shaft connected to a driving nut at the top of the apparatus. This nut was held on a 1/2" x 20 screw, such that the sphere moved approximately 1.27 mm for each 360° turn of the nut.

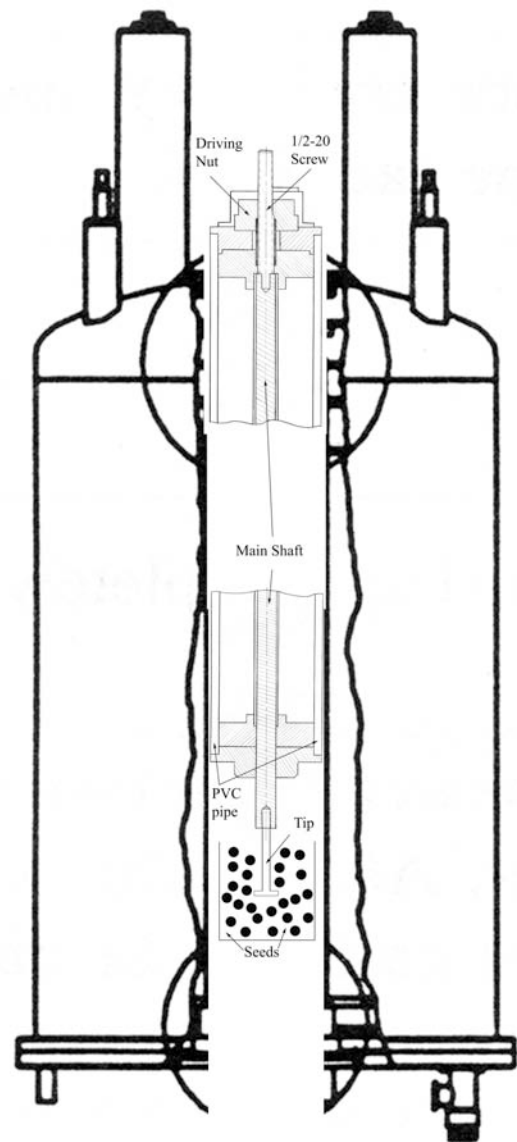


Figure 1. Experimental apparatus with cross-section of seeds. *Courtesy of Dr. Igor Veretennikov.*

Image Sequence Acquisition

Five different experiments were run, varying seed size (poppy seeds or mustard seeds), step size (~0.635 mm or ~0.070 mm displacements), and initial condition. Experiments were either started at the top of the cylinder, providing a series of downward plunges followed by withdraw steps, or from the bottom of the cylinder, making withdraw steps only.

Using a spin echo pulse sequence, proton density contrast between seeds and air was achieved using a repetition time of 500 ms and echo time of 14 ms. The square field of view was

6.0 cm per side, two averages were made, and total time for one scan was 8 min 32 sec. The reconstructed image matrix was 512 x 512 px.

Axial slices at varying depths were used as references when determining the slice scheme, which was composed of two vertical slices with slice thickness 1.0 mm. These slices were chosen such that they passed through the center of the sphere and avoided fringe fields. Once the slice scheme was chosen, sphere displacement began. At the beginning of each day, an initial scan was taken before any displacements were made. After each successive displacement, another image was acquired.

For experiments in which the sphere started at the top of the cylinder and was driven downward, this sequence of events was continued until the sphere was sufficiently far enough from the bottom of the cylinder to avoid wall effects (~1.0 cm from the bottom). The seeds were then allowed to relax overnight before beginning withdraw motions. For experiments in which the sphere began at the bottom of the cylinder and underwent withdraw only, seeds were allowed to relax overnight before beginning any motions.

At times, displacement of the plunger caused collapses located far from the sphere, resulting in large vertical motion of seeds. While all images were processed, those containing such collapses were removed before the final averaging stages of image analysis, as collapses were random events. There were not enough images with collapses to average together (shorter experiments usually had less than 5 collapse images, which is far too few to average).

Image Analysis and Particle Image Velocimetry

Particle Image Velocimetry (PIV) was used to determine seed displacements relative to the sphere. Before images were processed using PIV, spheres were "filled" with a circle of

seeds. The same circle was used for the entire image sequence, and this was found to greatly reduce noise within the actual sphere and clarify the region surrounding the sphere.

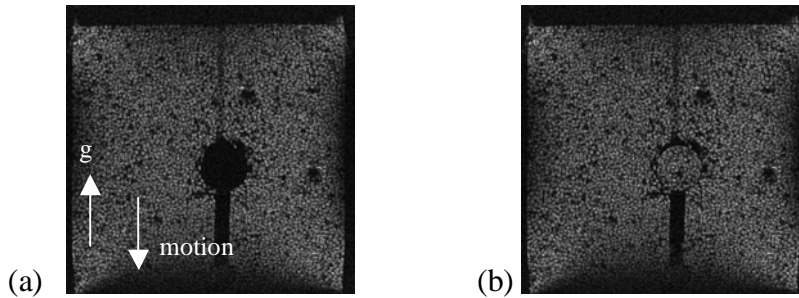


Figure 2. (a) Example of image before filling. (b) Example of filled image.

PIV cannot track individual seeds, so it divides an image into several small sections. For poppy seeds, this was a square with 30 px sides (~3.53 mm, matrix size 512 x 512 and FOV 6.0 cm), and for mustard seeds a square with 40 px sides (~4.69 mm). To determine displacement of a section, it was shifted around in the next image and correlated to each section of that image. A correlation matrix was produced after a section had been shifted around the entire region, and the maximum correlation indicated the most probable displacement of seeds between the two scans [4]. Figure 3 illustrates the basic principle of PIV. This procedure was performed for all sections of the entire image sequence, and the smallest detectable motion was ± 1 px.

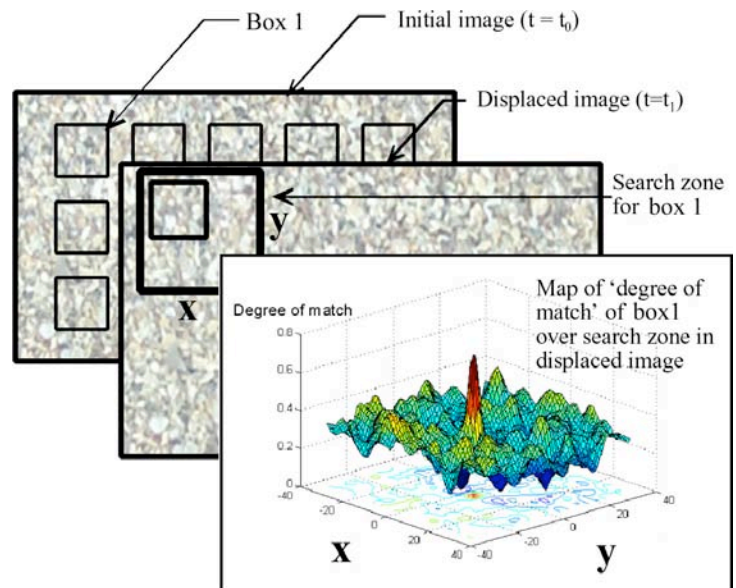


Figure 3. Basic principle of PIV. The original image is divided into sections then shifted around in the following image. The correlation matrix is created, and in this case the maximum correlation is well defined [4].

RESULTS AND DISCUSSION

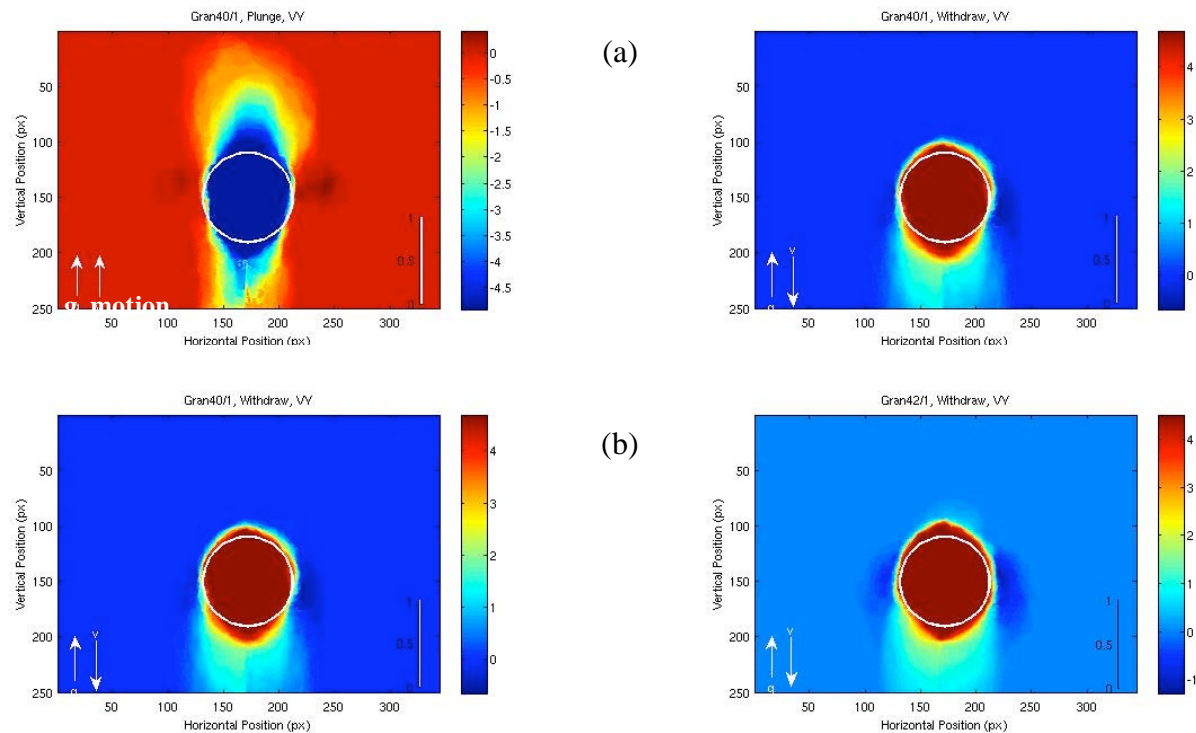
Results

Table 1 below is a summary of all seven runs.

Table 1. Summary of experiments. * Indicates a mistake in setting image sequence parameters; this scan was not processed but image sequence was kept. ^ Indicates a scan that has not completed PIV processing at the time of this report, and thus was not averaged.

Experiment	Seed	Step Size (mm)	Initial Location (top or bottom)
Gran 40	Poppy	0.635	Top
Gran 41*	Poppy	0.635	Bottom
Gran 42	Poppy	0.635	Bottom
Gran 43	Mustard	0.635	Bottom
Gran 44	Mustard	0.635	Top
Gran 45	Poppy	0.070	Bottom
Gran 46 ^	Mustard	0.070	Bottom

As seeds were subject to both displacements caused by the sphere itself and random collapses of arches and settling, averages were performed for each run, and calculated in a moving reference frame. By using a moving reference frame, average displacements were those *relative to the sphere*. Several averaged images are below (Figure 4).



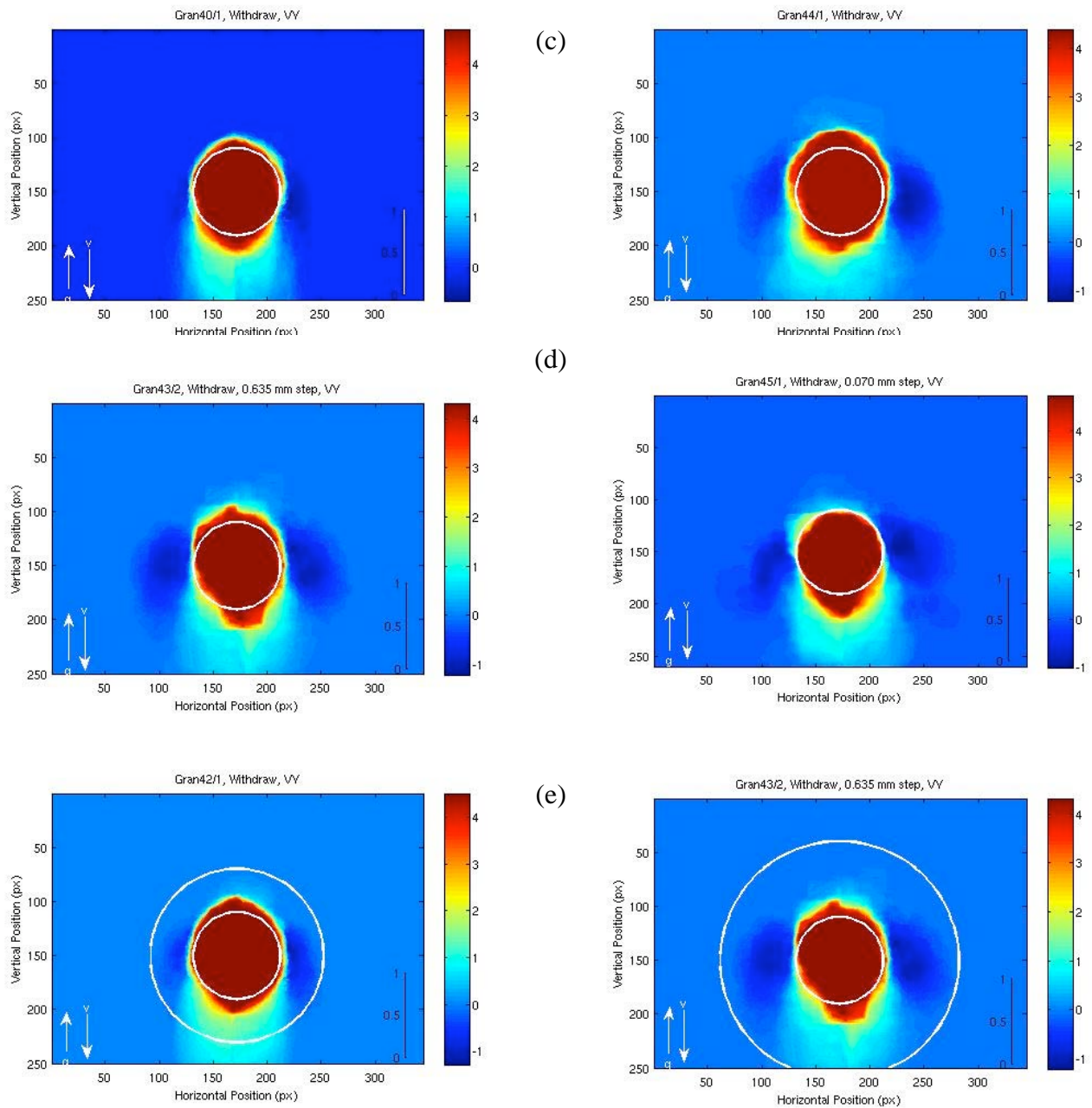


Figure 4. Average vertical displacements for several experiments. Small white circles indicate the location of the sphere, which is approximately 1 cm in diameter. (a) Gran40, Slice 1. The left image represents the downward plunging motion, while the image on the right is withdrawal motions only. (b) The left image is Gran40 withdrawal motion, and the right image is Gran42. These two runs only differ by initial condition; Gran40 included plunging motions, while Gran42 did not. (c) The left image is Gran40 withdrawal motion (poppy seeds), and the right image is Gran44 withdrawal motion (mustard seeds). (d) The left image is Gran43 (mustard seeds, 0.635mm steps), and the right is Gran 45 (mustard seeds, 0.070mm steps). (e) The left image is Gran42, with larger circle indicating a layer 10 poppy seeds deep. The right image is Gran43, with larger circle indicating a layer 5 mustard seeds deep.

Assessment of Granular Flow Using Analytical Solutions for Fluids

Vertical profiles were much easier to compare and contrast; for this reason they were used in analysis. To better understand the granular flow observed in this experiment, the plunging motion of Gran40 was compared to the analytical solutions for viscous and inviscid fluid flow, which are already well known and described. The solution for steady, inviscid, incompressible flow around a sphere is given by Bertin [5]. After being normalized and modified to fit the conditions of this experiment, such that flow is zero when distance from the center of the sphere is infinite the solution becomes:

$$v_r / v_0 = (a^3/r^3)$$

where a is the radius of the sphere and r is the distance from the center of the sphere. The solution for very viscous flow around a sphere is given by Acheson [6]; after normalization and modifications to fit the conditions of the experiment as before, the solution becomes:

$$v_r / v_0 = a*(3r^2 - a^2) / r^3$$

Figure 5 shows the result of the comparison.

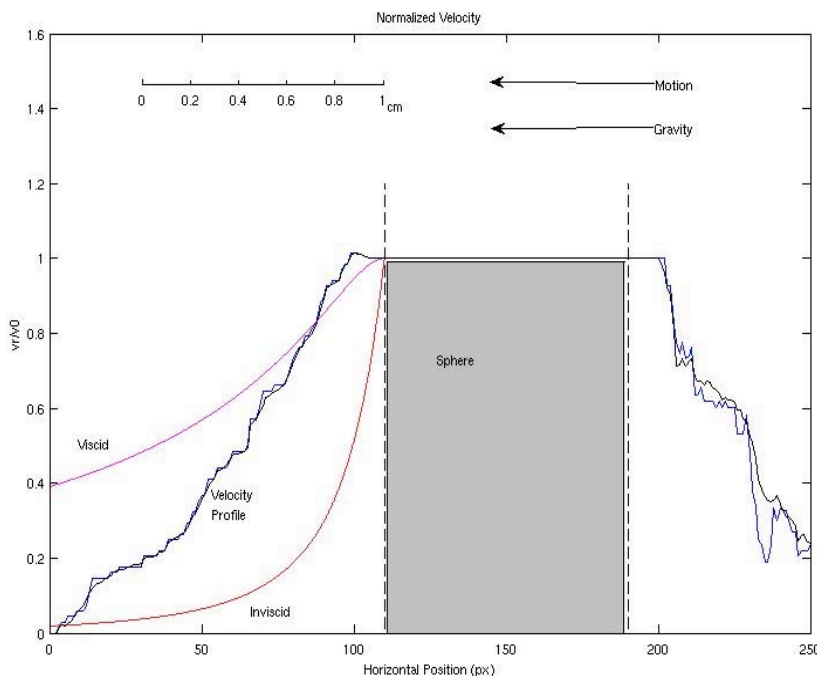


Figure 5. Plot of the normalized velocity for Gran40, plunging motion, as well as solutions for viscous and inviscid fluid flows. The two dashed lines appear at 110 and 190 px, the locations of the edge of the sphere.

The region near the sphere most closely represents viscous fluid flow, but quickly undergoes a phase change. Farther from the sphere, the granular flow is closer to inviscid fluid flow, although this is a weak representation of inviscid flow. However, it is evident that granular flow heavily depends on distance from the sphere.

Discussion of Conclusions

While granular flow for plunging and withdrawing is fundamentally the same, in that seeds flow in response to the sphere displacing them, there are significant differences. Plunging compresses seeds, this applied pressure is the cause of granular flow. When withdrawing, pressure builds up behind the sphere. Holes form, but there is no adhesion between seeds, so they collapse only when the applied pressure is too great for seeds to overcome. Plunging causes greater motion at the front of the sphere, where it applies pressure. This area is significantly decreased when withdrawing.

It was found that granular flow depended on initial condition and, more profoundly, on seed size. When comparing experiments that vary initial condition only, it is immediately noted that fully plunging before withdrawing reduces the physical region of motion. Merely withdrawing affects a much larger area, and causes seed displacements at distances farther from the sphere, for both mustard and poppy seeds. One possible explanation is that the plunging motion creates a dual-layered system of seeds. Seeds near the walls of the cylinder move very little—partial-voxel distances that cannot be detected by PIV. This region retains its relatively high density, while seeds surrounding the plunger are disturbed, moving greater distances, and rearrange, creating a lower-density region. When withdrawing begins, it is only this lower-density region that undergoes motion.

Mustard seeds and poppy seeds showed two different granular flow tendencies. Mustard seeds filled cavities as soon as enough seeds had expanded that they could flow and fill the vacancy. Poppy seeds, however, created large vacancies, which persisted until large collapses filled the cavity. These collapses were random and were directly caused by movement of the plunger. These cavities appeared during the day, so it is assured that they are not caused by overnight relaxations. Step size produced small but noticeable differences, in that *smaller* steps (0.070 mm vs. 0.635 mm) were associated with *larger* cavities.

Dependence on seed size was also noticeable when comparing how quickly motion decays. Displacement of the sphere affected a maximum layer of mustard seeds approximately five seeds deep; while poppy seeds experienced motion through a layer ten seeds deep.

A logical next step would be to study motion caused by large collapses. However, as they appear randomly, an immense number of images would be required to assure enough collapse images would be available for averaging. Another interesting investigation would include modifying PIV methods to detect partial-voxel motions; this could provide much better information about motion decay.

ACKNOWLEDGEMENTS

I owe many thanks to Dr. Igor Veretennikov for his assistance, guidance, and patience. The knowledge he has imparted about MRI, granular materials, and research methods has been invaluable. I also wish to thank Professor Umesh Garg, through whom I was able to participate in Notre Dame's REU program and carry out this research. Lastly, I am grateful to the National Science Foundation for its financial support.

LITERATURE CITED

- [1] Jaeger, H.M., Nagel, S.R., "Physics of the Granular State," *Science* **255** (1992) 1523-1531.
- [2] Jaeger, H.M., Nagel, S.R., "Granular solids, liquids, and gases," *Rev. Mod. Phys.* **68** (2004) 1259-1273.
- [3] Corwin, E.I., Jaeger, H.M., Nagel, S.R., "Structural signature of jamming in granular media," *Nature* **435** (2005) 1075-1078.
- [4] White, D.J., Take, W.A., Bolton, M.D., "Measuring soil deformation in geotechnical models using digital images and PIV analysis," *10th International Conference on Computer Methods and Advances in Geomechanics* (2001) 997-1002.
- [5] Bertin, J.J., *Engineering Fluid Mechanics* (1984) 189-190.
- [6] Acheson, D.J., *Elementary Fluid Dynamics* (1990) 223-225.